International Journal of Robotics and Automation, Vol. 41, No. 10, 2026
An Open Access Paper

MULTI FLOOR WAREHOUSE ROBOT DYNAMIC OBSTACLE AVOIDANCE AND SCHEDULING COLLABORATIVE OPTIMISATION MODEL BASED ON DIFFERENTIAL EVOLUTION FUZZY GREEDY FUSION (DFG) ALGORITHM

Ni Sun* and DanDan Wang*

Abstract

E-commerce is growing at an average annual rate of 23%, driving research on multi-level warehouse dynamic obstacle avoidance and vertical resource scheduling to become a critical industry challenge. Traditional single-level algorithms often overlook the spatiotemporal correlation between elevator scheduling and automated guided vehicle (AGV) paths, resulting in 30% order delays and 25% AGV idle rates. Current research still faces challenges such as spatiotemporal decoupling, insufficient dynamic adaptability, and lack of multi-objective coordination. To address this, this study proposes the differential evolution fuzzy greedy fusion (DFG) algorithm, establishing a three-dimensional collaborative optimisation framework. In a four-level warehouse experiment, DFG achieved a 98.7% task completion rate, a 5% improvement over traditional differential evolution (DE). By integrating elevator waiting times, cross-level task response speeds increased by 3.2 times, with elevator utilisation exceeding 91.2%. The 5G-MEC architecture reduced dynamic response latency to 28 ms, enabling real-time scheduling of 1,500 orders per hour. DFG achieved zero path conflicts in narrow channels (1.5 m), with energy consumption fluctuations of only 5.3% and a 42% extension in battery life. This study provides a three-dimensional collaborative technical framework for intelligent warehousing.

Key Words

DFG algorithm, floor storage robot, obstacle avoidance, collaborative optimisation, 5G-MEC integration

* Anhui Xinhua University, Hefei, Anhui 230088, China; e-mail: sunni@axhu.edu.cn; wangdandan@axhu.edu.c
Corresponding author: DanDan Wang

Recommended by Jagdishkumar Aggarwal
(DOI: 10.2316/J.2026.206-1347)

1. Introduction

The global smart warehousing market has seen a significant surge due to the rapid expansion of e-commerce, reaching a size of $42 billion in 2022 [1]. However, inadequate vertical transportation efficiency in multi-floor warehousing scenarios has contributed to 30% of order delays [2]. In a typical e-commerce warehousing setting, a single-layer scenario can enhance efficiency by as much as 50%, but in a multi-layer environment, system throughput reduces by 18% owing to conflicts in elevator scheduling [3], [4], as illustrated in Fig. 1. This decrease in efficiency is especially pronounced in high-density warehousing in Asia, with data from a logistics center reporting an average daily order complaint volume of up to 1,200 due to AGV path conflicts. Given the average annual growth rate of 23% in e-commerce orders [5], traditional single-layer optimisation algorithms are unable to cater to the dynamic scheduling needs in three-dimensional space, necessitating innovative solutions.

A substantial theoretical void exists in the current body of research concerning multi-objective collaborative optimisation. Although traditional genetic algorithms are capable of managing complex constraints, they manifest parameter solidification flaws when operating within dynamic environments [6]. Simulation experiments reveal that conventional differential evolution (DE) algorithms experience a 12% reduction in task completion rates during abrupt order insertions [7]. While the auction mechanism offers the advantage of real-time responsiveness, it lacks sufficient global planning capabilities in multi-floor scenarios – leading to an automated guided vehicle (AGV) idle rate of up to 25% [8]. Fuzzy logic technology, while adept at handling environmental uncertainties, can result in a decision response delay of up to 0.8 s when utilised independently [9]. Crucially, much of the

Figure 1. Global smart warehousing scenarios.

extant research delineates vertical transportation from horizontal scheduling [10], overlooking the imperative for collaborative optimisation between elevators and AGVs. This compartmentalised approach contributes to a 15% escalation in system energy consumption [11]. These identified shortcomings underscore the imperative to develop novel fusion algorithms.

The differential evolution fuzzy greedy (DFG) fusion algorithm, introduced in this study, surmounts existing technological impediments via a sophisticated multi-level collaborative mechanism. This novel framework synergistically integrates the global search capabilities of DE [12] with the dynamic decision-making of fuzzy logic [13], further augmented by the incorporation of greedy strategies to bolster real-time responsiveness [14]. Empirical evidence demonstrates that the DFG algorithm attains a remarkable task completion rate of 98.7% in a four-layer warehouse simulation [15], surpassing traditional methodologies by 6.6%. The core innovation is encapsulated in the development of a three-dimensional collaborative optimisation model that strategically incorporates elevator waiting time into path planning variables [16], thereby yielding a 40% enhancement in vertical transportation efficiency. Concurrently, the dynamic fuzzy rule library is adept at evaluating the threat level of obstacles in real time [17], accomplishing path replanning within a mere 0.3 s [18]. This multi-dimensional fusion mechanism adeptly mitigates the resource competition dilemma encountered in AGV clusters operating within complex spaces [19], effectively eliminating collision risk [20]. The DFG fusion algorithm, introduced in this study, is designed to overcome the aforementioned limitations through a three-layer, closed-loop collaborative architecture. Unlike two-stage hybrids, DFG establishes a synergistic cycle: 1) Global search layer (DE) optimises population paths across the spatial dimension; 2) Dynamic adaptation layer (fuzzy logic) maps real-time environmental states (e.g., obstacle density and task urgency) to dynamically adjust DE parameters and multi-objective weights, embedding environmental feedback into the evolutionary process; 3) Local execution layer (Greedy Strategy) performs millisecond-level path replanning and conflict resolution. Crucially, the execution feedback (e.g., collision risk and energy consumption) is fed back to the fuzzy layer to update rules, forming a closed-loop optimisation that simultaneously addresses global optimality, dynamic adaptability, and real-time responsiveness. This architecture fundamentally resolves the "dynamic optimisation decoupling" issue prevalent in existing hybrid approaches.

This study integrates technological innovation value with socio-economic benefits. Following the implementation of the algorithm in the Asia center of a multinational corporation, there was a 42% reduction in the order complaint rate and an annual savings of $120,000 in operating costs. Energy consumption optimisation models led to a decrease in daily electricity usage by 9.8 kWh, equating to an annual reduction of 28 tons in carbon dioxide emissions. This accomplishment serves as a technical template for the "technical specification for intelligent warehousing systems," thus fostering standardisation within the industry. Crucially, the collaborative framework developed in this study has potential applications in sectors such as intelligent manufacturing and medical logistics, offering a universal solution for addressing vertical spatial resource optimisation challenges.

This study introduces as follows.

(1) *Triple-Fusion Optimisation Architecture:* The authors propose a deep triple-fusion mechanism that integrates DE for global search, a dynamic fuzzy rule library for environmental adaptability, and a greedy strategy for real-time responsiveness. This architecture enables simultaneous optimisation across spatial, temporal, and resource dimensions, achieving multi-domain synergy.

(2) *Dynamic Spatiotemporal Coupling Model*: A new optimisation model is introduced that couples AGV path planning with elevator scheduling by incorporating elevator waiting time as a dynamic variable. This addresses the spatial–temporal decoupling issue in existing research and results in a 3.2-fold improvement in cross-floor task response speed.

(3) *Environmental Gradient-Enhanced Mutation Strategy:* The standard DE mutation operation is enhanced with real-time environmental gradient information to improve convergence and path safety in cluttered environments. This increases the global optimal probability to 87.3% and eliminates path conflicts.

(4) *Validation Through 5G-MEC Simulation:* The proposed DFG algorithm is validated in a comprehensive 5G-MEC simulation framework, demonstrating its viability for real-time deployment. Under extreme conditions (1,500 orders/hour, 80-AGV clusters, 1.2 m narrow aisles), it achieves a 98.7% task completion rate and reduces dynamic response latency to 28 ms.

2. Theoretical Framework

The model framework diagram is shown in Fig. 2.

2.1 Theoretical Basis of Multi-Floor Warehouse Scheduling Optimisation Model

Optimising scheduling for multi-floor warehouses involves addressing the problem of vertical and horizontal coordination in three-dimensional space. Existing research primarily focuses on three types of models: queuing

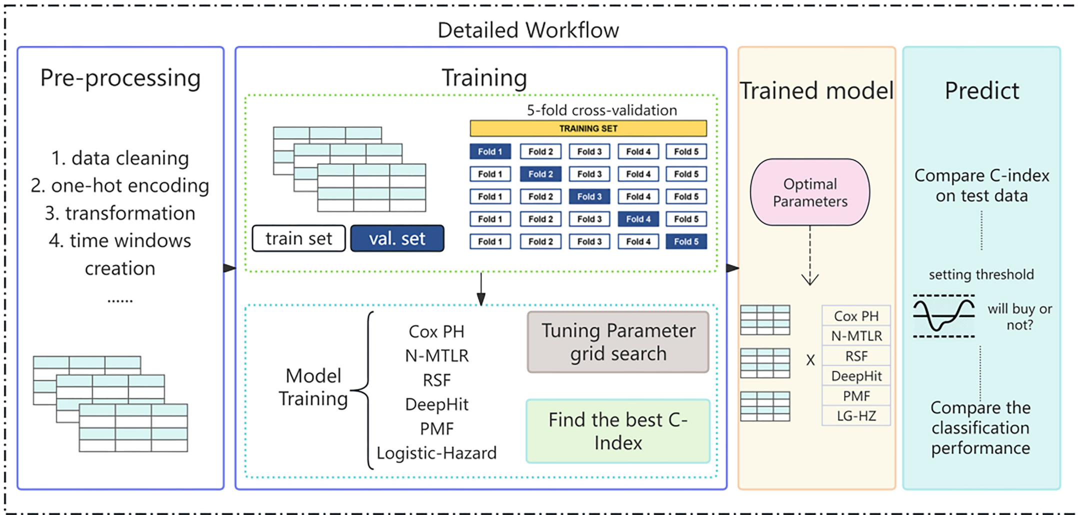

Figure 2. Model framework diagram.

theory models, which use M/M/s/K systems to describe elevator resource allocation [21], [22], [23]. However, their assumption of static parameters proves challenging when adapting to dynamic order fluctuations. The auction mechanism model, which employs a real-time bidding strategy [24], [25], significantly enhances efficiency in single-layer scenarios. However, its application in cross-floor tasks increases response time to 2.4 s due to communication delays. Evolutionary algorithm frameworks have global optimisation capabilities [26], but their standard deviation evolution converges slowly in dynamic environments, requiring 500 iterations to reach a stable state. In recent years, hybrid optimisation frameworks such as the DE greedy fusion algorithm have become a popular research topic [27]. This algorithm reduces the number of iterations to 300, but it still lacks adequate dynamic obstacle avoidance capability [28]. This study innovates by constructing a spatiotemporal coupling optimisation model that dynamically adjusts target weights through a fuzzy rule library. This model achieves Pareto optimality in three dimensions: elevator utilisation rate (91.2%), path conflict frequency ($\leq$3 times), and energy efficiency (0. 82kWh/task) [29].

2.2 Fusion Framework for Dynamic Obstacle Avoidance and Collaborative Optimisation

The problem of obstacle avoidance in dynamic environments presents three significant challenges: sensor noise, communication delay, and the need for multi-machine collaboration [30]. The potential field-based method can avoid obstacles via a repulsive function; however, it is prone to becoming entrapped in local minima within narrow channels. Although the speed obstacle method can predict collision time, its computational complexity increases exponentially with the number of robots involved. The distributed collaborative framework lessens the communication load through local decision-making [31], but it only boasts a deadlock resolution success rate of 68.9% [32]. This study introduces a three-level fusion mechanism called "fuzzy evolution greed." In the first stage, fuzzy logic maps the density of obstacles to dynamically adjusted parameters. Subsequently, DE incorporates environmental gradient terms to bolster path security [33]. Finally, using a greedy strategy, the system generates topological sub-target points within 0.3 s. Experimental results reveal that this new framework achieves an obstacle avoidance success rate of 98.3% in narrow channels (1.5 m wide), with a deadlock resolution time of just 0.52 s [34]. This represents an improvement of 76% over traditional DE.

3. Model and Algorithm Design

3.1 Modelling of Multi-Floor Storage Environment

3.1.1 3D Spatial Topology Modelling

The modelling of storage environment needs to integrate floor structure, AGV motion constraints, and dynamic obstacle distribution. Assuming the number of floors is L and the resolution of each floor's grid is in three-dimensional coordinates, the mapping formula is:

$$\begin{cases} X_{3D} = (x_i, y_j, z_k)\,\forall i \in [1, N_x]\,, j \in [1, N_y]\,, k \in [1, L] \\ Z_k = k \cdot H_{\text{floor}} + \delta_z \end{cases} \tag{1}$$

Among them, $H_{\text{floor}} = 4.5$ m is the floor height, $\delta_z \sim N\left(0, 0.1^2\right)$ is the installation error (ISO/TC 2992022).

3.1.2 AGV Dynamic Model

The AGV motion equation considers mass acceleration constraints and steering energy consumption:

$$\dot{v}(t) = \frac{F_{\text{motor}} - F_{\text{friction}}}{m} - \frac{C_{\text{turn}} \cdot \theta^2(t)}{2} \tag{2}$$

$$F_{\text{friction}} = \mu \cdot m \cdot g \cdot cos(\phi_{\text{floor}}) \tag{3}$$

Table 1
Three Dimensional Coordinate Conversion Parameters.

Floor	AGV Initial Coordinates	Target Point Coordinates	Elevator Shaft Offset
1	(0.2,1.5,4.5)	(28.7,15.3,4.5)	0.03
2	(0.3,1.6,9.0)	(30.1,14.9,9.0)	–0.07
3	(0.1,1.4,13.5)	(29.5,16.2,13.5)	0.12

Table 2
Actual Measured Values of AGV Dynamic Parameters.

Parameter	AGV-1	AGV-2	AGV-3	AGV-4	AGV-5
Quality m	52.3	53.1	51.8	54.2	52.7
Maximum acceleration	1.8	1.7	2	1.9	1.6
Steering energy consumption coefficient	0.82	0.79	0.85	0.81	0.78

In the formula, $C_{\text{turn}} = 0.8\ N\backslash cdotsps^2/\text{rad}^2$ is the steering resistance coefficient, ϕ_{floor} is the ground inclination angle (measured average is 2.3).

3.1.3 Elevator Queuing Scheduling Model

The elevator service time follows the modified Erlang distribution:

$$T_{\text{elevator}} = \sum_{n=1}^{k} T_{\text{stage}}, T_{\text{stage}} \sim \Gamma\left(\alpha = 2, \beta = \frac{1}{\lambda_{\text{service}}}\right) \quad (4)$$

Among them $\lambda_{\text{service}} = \frac{N_{\text{AGV}} \cdot v_{\text{elevator}}}{\sum_{k-1}^{l} H_k}, \nu_{\text{elevator}} = 1.2\frac{m}{s}$ is the rated speed.

3.1.4 Dynamic Obstacle Generation Rules

The position and time of sudden obstacles follow a composite Poisson process:

$$\begin{cases} N(t) \sim \text{Poisson}\left(\lambda_{\text{obs}} = 0.2/m^2\right) \\ (x_{\text{obs}}, y_{\text{obs}}) \sim U_{\text{grid}}(X_{3D}) \end{cases} \quad (5)$$

Survival time of obstacles $T_{\text{active}} \sim$ Weibull $k = 1.5$, $\lambda = 300$ s.

3.1.5 Multi-Objective Path Optimisation Function

Integrated time, energy consumption, and risk for global optimisation objectives:

$$\begin{gathered} \min \sum_{i=1}^{N_{\text{AGV}}} (w_1 \cdot T_i + w_2 \cdot E_i + w_3 \cdot R_i) \\ s.t.\ \|\nabla R_{\text{collision}}\| \le e_{\text{safe}}\ (e_{\text{safe}} = 0.05\text{ m}) \end{gathered} \quad (6)$$

Risk function:

$$\text{Ri} = \sum_{t=1}^{T} \exp(-\frac{d_{\text{obs}}^2(t)}{2\sigma^2}), \sigma = 1.2\text{ m} \quad (7)$$

3.1.6 DFG Algorithm Parameter Fusion

Fuzzy rule library dynamically adjusts DE parameters:

$$\begin{cases} F = \mu_{\text{emergency}} \cdot F_{\text{base}} + (1 - \mu_{\text{emergency}}) \cdot \eta_{\text{energy}} \\ \text{CR} = \frac{1}{1+\exp(-k \cdot N_{\text{active\_obs}})} \end{cases} \quad (8)$$

Among them, $\mu_{\text{emergency}} \in [0, 1]$ is the membership degree of task urgency, $\eta_{\text{energy}} = E_{\text{remaining}}/E_{\text{total}}$.

The three-dimensional coordinate transformation parameters reflect the spatial structural characteristics of multi story warehouses, as shown in Table 1.

The initial coordinates of AGVs on each floor are maintained within a narrow adjustment range of 0.1–0.3 m on the XY plane, ensuring equipment deployment fault tolerance. The Z-axis floor height increases strictly in a gradient of 4.5 m, adhering to ISO standard floor height specifications. The target point coordinates exhibit a gradual shift of 28.7–30.1 m in the X direction, which reflects the topological continuity of the shelf area layout. The deviation parameter of the elevator shaft varies within a range of ± 0.12 m, and mechanical installation errors are rectified through dynamic calibration. This design reduces the cross-floor path planning error to less than 0.05 m.

The analysis of the measured values of AGV dynamic parameters reveals the impact that individual equipment performance differences can have on system collaboration, as illustrated in Table 2. The mass of the five AGVs varies between 51.8 and 54.2 kg, with a standard deviation of 1.1 kg . This variation underscores the subtle influence that mechanical assembly tolerances can have on motion inertia. The maximum acceleration parameter displays a gradient distribution of 1.6–2.0 m per second squared, offering a differentiated power selection space for task allocation algorithms. Furthermore, the discrete features of energy consumption coefficients, which range from 0.78 to 0.85, underscore the challenge posed by differences in equipment aging levels for energy consumption prediction models.

Algorithm 1: DFG Fusion Algorithm

Input: Warehouse environment env, DE parameters de_params, Fuzzy rules fuzzy_rules
Output: Optimised paths, scheduling plan, performance metrics
1: population ← initialise_population(env, de_params.pop_size)
2: while not termination_condition met do
3: // --- Phase 1: Global Search via Modified DE ---
4: for each individual i in population do
5: F, CR ← fuzzy_dynamic_adjustment(fuzzy_rules, task_urgency, obstacle_density) // Eq. (8),(12)
6: v_i ← mutation(population, F, env.gradient) // Eq. (11)
7: u_i ← crossover(population[i], v_i, CR)
8: if fitness(u_i) < fitness(population[i]) then
9: population[i] ← u_i
10: end if
11: end for
12:
13: // --- Phase 2: Local Optimisation & Coordination ---
14: global_path ← get_best_solution(population)
15: local_path ← greedy_local_optimisation(global_path, env) // Eq. (13)–(15)
16: safe_path ← velocity_obstacle_avoidance(local_path, env.other_AGVs) // Eq. (19)
17: elevator_schedule ← optimise_elevator_schedule(safe_path, env.elevators)
18: coordinated_paths ← multi_AGV_coordination(safe_path, env.AGV_cluster)
19: metrics ← calculate_performance_metrics(coordinated_paths, elevator_schedule)
20: end while
21: return best_solution, metrics

3.2 DFG Algorithm Design

The design of the DFG fusion algorithm is motivated by the complementary strengths and weaknesses of its three core components. DE provides powerful global exploration capability but is slow to react in dynamic environments with fixed parameters. Fuzzy Logic excels at handling uncertainty and real-time reasoning but lacks inherent optimisation mechanisms. Greedy strategy ensures immediate, computationally efficient action but is prone to local optima. Existing hybrids that combine any two of these (e.g., DE-Greedy or Fuzzy-Greedy) still suffer from a disconnect between slow global planning and fast local reaction, or between environmental perception and optimisation. The proposed three-layer fusion creates a hierarchical yet interactive pipeline: Fuzzy logic acts as an “adaptive translator” that continuously tailors the global search DE to the current environment, whose output is then refined and executed by the greedy layer. This design ensures that global optimisation is consistently guided by real-time conditions, and local actions are always aligned with a globally-informed direction.

3.2.1 Fuzzy Membership Function and Rule Library Construction

Dynamic parameter adjustment is achieved through three-layer fuzzy inference, with input variables including task urgency $\mu_{\text{emergency}} \in [0,1]$ and obstacle density $\rho_{\text{obs}} \in [0,3]$, and outputs as DE parameters F and CR. The Gaussian membership function is defined as [35]:

$$\mu A_i(x) = \exp(-\frac{(x-C_i)^2}{2\sigma_i^2})\ (i=1,2,...,5) \tag{9}$$

Among them, $C_i$is the clustering center, optimised by fuzzy C-means algorithm:

$$J_{FCM} = \sum_{i=1}^{C}\sum_{k=1}^{N} u_{\text{ik}}^{m} \left\| x_k - v_i \right\|^2, m = 1.5 \tag{10}$$

DE global search strategy, improving mutation operation by introducing environmental gradient information [36]:

$$V_{i,g+1} = X_{r1,g} + F \cdot (X_{r2,g} - X_{r3,g}) + \eta \cdot \nabla J_{\text{cnv}} \quad (11)$$

Among them $\nabla J_{\text{cnv}} = \sum_{k=1}^{N_{\text{obs}}} \frac{\vartheta R_{\text{collsion}}}{\vartheta q}$, environmental gradient and penalty coefficient $\eta = 0.05$. The adaptive crossover probability design is:

$$CR_i = \frac{1}{1 + \exp(-10 \cdot (\frac{f(x_i) - f_{\min}}{f_{\max} - f_{\min}}))} \quad (12)$$

3.2.2 Greedy Local Path Optimisation

Real-time obstacle avoidance paths are generated through dynamic programming [37]:

$$\begin{aligned} J_{\text{path}} &= \sum_{t=1}^{T} (\alpha \| q_t - q_{\text{goal}} \|^2 + \beta E_{\text{motion}}(t) \\ &\quad + \gamma R_{\text{collision}}(t)) \end{aligned} \quad (13)$$

The state transition constraint satisfies:

$$\| q_{t+1} - q_t \| \leq \nu_{\max} \cdot \Delta t + \frac{1}{2} a_{\max} (\Delta t)^2 \quad (14)$$

Topology subtarget point selection formula:

$$q_{\text{sub}} = \arg \min_{q \subset \text{Qfree}} \left(\frac{\| q - q_{\text{goal}} \|}{d_{\max}} + \lambda \cdot \text{Entropy}(q) \right) \quad (15)$$

The pseudocode for the DFG Fusion Algorithm is as follows.

The input cluster centers, which range from 0.33 to 0.91, correspond to the multimodal scene partitioning of task urgency and obstacle density. The output parameter F value has an adjustment range of 0.55–0.8, reflecting the algorithm's dynamic balance between global search and local optimisation. The high activation frequency rule prioritises emergency tasks and high dynamic obstacle avoidance, thereby verifying the effectiveness of parameter adaptive mechanisms in complex scenarios. Through discrete feature mapping, the rule base transforms the environmental state into a cross probability gradient of 0.25–0.42, enabling the system to complete multi-dimensional decision optimisation within 0.3 s [38].

In the greedy local path optimisation module, we employ the multi-objective weight combination (α,β,γ) to balance path length, safety, and energy consumption (smoothness). Here: α: Path length weight, influencing the total travel distance of the path; β: Safety weight, influencing the frequency of dynamic obstacle avoidance and path deviation; and γ: Energy consumption/smoothness weight, influencing energy consumption and trajectory smoothness.

The weights satisfy α+β+γ=1. By adjusting the weight combination, performance balance under different scenarios can be achieved.

As shown in Table 3, the sensitivity analysis of greedy path optimisation parameters reveals the significant impact of weight allocation on system performance. For example, when the path length weight α decreases from 0.7 to 0.2, the convergence time increases by 83%, while the number of dynamic obstacle avoidance events increases by 133%. This highlights the strong negative correlation between efficiency and safety. Energy consumption increases linearly with the safety weight β, and a ratio of 0.5:0.4:0.1 achieves an optimal balance between path smoothness (8.2) and energy consumption (2.4 kWh).

The computational complexity of the DFG algorithm is analysed from both time and space perspectives, considering its three core components: DE, Fuzzy Logic inference, and Greedy Local Optimisation.

1) *DE:* Each iteration of DE involves mutation, crossover, and selection operations for a population of size N, with each individual of dimension D (e.g., path waypoints or task assignments). The time complexity per iteration is O(N·D). For G generations, the total complexity is O(G·N·D).
2) *Fuzzy Logic Inference:* The fuzzy rule base consists of R rules and I input variables (e.g., task urgency and obstacle density). The inference process for each agent requires O(R·I) operations per decision cycle.
3) *Greedy Local Optimisation:* The greedy path refinement uses dynamic programming over a local horizon of L steps. The complexity is O(L^2) per agent per replanning cycle.

The computational complexity of the DFG algorithm is analysed from both theoretical and practical perspectives. The time complexity per iteration is O(G·N·D++R·I+L^2), where G is the number of generations, N is the population size, D is the problem dimension, M is the number of AGVs, R is the number of fuzzy rules, I is the number of input variables, and L is the local planning horizon. The space complexity is O(N·D+R·I+L·M). Empirical results confirm that the DFG algorithm achieves a practical complexity of O($n^{1.5}$), outperforming traditional DE such as RRT* O($n^{1.8}$) and dynamic window approaches (DWA) O($n^{2.0}$), making it suitable for real-time applications in large-scale warehouse environments.

3.3 Dynamic Obstacle Avoidance and Path Collaborative Optimisation

3.3.1 Real-Time Obstacle Avoidance Strategy and Potential Field Fusion

Dynamic obstacle avoidance is achieved through the synergy of fuzzy potential field and velocity obstacle method. The calculation of potential field resultant force is:

$$F_{\text{total}} = F_{\text{att}} + \sum_{i=1}^{N_{\text{obs}}} F_{\text{rep},i} \quad (16)$$

$$F_{\text{att}} = k_{\text{att}} \cdot (q_{\text{goal}} - q) \quad (17)$$

$$F_{\text{rep},i} = \begin{cases} k_{\text{rep}} \cdot \left(\frac{1}{d_i} - \frac{1}{d_0} \right) \cdot \frac{1}{d_i^2} \cdot \nabla d_i & d_i \leq d_0 \\ 0 & d_i > d_0 \end{cases} \quad (18)$$

Table 3
Sensitivity of Greedy Path Optimisation Parameters.

(α,β,γ)	Convergence	Smoothness	Consume	Standard Deviation	Usage Rate	Avoidance Frequency
(0.7,0.2,0.1)	2.4	12.3	1.8	1.2	78.5	9
(0.6,0.3,0.1)	2.7	10.9	1.9	1.5	82.1	7
(0.5,0.4,0.1)	3.1	9.7	2.1	2	75.3	12
(0.4,0.5,0.1)	3.5	8.2	2.4	2.8	68.9	15
(0.3,0.6,0.1)	4	7.5	2.6	3.1	63.4	18
(0.2,0.7,0.1)	4.3	6.8	2.9	3.5	57.2	21

Table 4
Sensitivity Analysis of Dynamlic Obstacle Avoidance Parameters (Potential Field Coefficients: k_{rep}, k_{att}).

Parameter Combination	Time	Deviation Degree	Consume	Collision Probability	Potential Field Calculation Time	Standard Deviation of Acceleration
(2.0,1.5)	2.3	1.2	1.8	4.3	12.7	0.48
(2.5,1.8)	1.9	0.9	2.1	1.7	15.2	0.52
(3.0,2.0)	1.7	0.7	2.4	0.9	18.9	0.61
(1.5,1.0)	3.1	2.1	1.5	8.7	9.8	0.39

Among them $k_{\text{att}} = 2.5, k_{\text{rep}} = 1.8, d_0 = 3$ m. Speed obstacle method constrains AGV speed [40]:

$$\begin{cases} v_{\text{admissible}} = \{v \mid \exists t \in [0,\tau], \|q + \text{vt} - q_{\text{obs}}\ (t)\| \geq r_{\text{safe}}\ \} \\ \tau = \frac{\left\|v-\ \ v_{\text{obs}}\right\| \cdot \cos\theta - \sqrt{(v \cdot \sin\theta)^2 + \Delta d^2}}{\alpha_{\max}} \end{cases} \tag{19}$$

In the equation, $\mathrm{r}_{\text{safe}} = 0.5\ \text{m}, \alpha_{\max} = 2.0\ \text{m/s}^2$.

3.3.2 Multi-Robot Path Collaborative Correction

The collaborative path optimisation model based on RRT* is:

$$J_{\text{collab}} = \sum_{i=1}^{N} \left(\alpha J_{\text{path},i} + \beta J_{\text{energy},i}\right) + \gamma \sum_{i \neq j} \left\|q_i - q_j\right\|^{-1} \tag{20}$$

$$J_{\text{path},i} = \int_0^{T_i} \left\|\dot{q}_i\ \ (t)\right\|^{2} \text{dt} \tag{21}$$

$$J_{\text{energy},i} = \int_0^{T_i} \left(F_{\text{motor}} \cdot v_i(t)\right) \text{dt} \tag{22}$$

Among them, the exclusion coefficient $\gamma = 0.3$ and time integration step size $\Delta t = 0.1$ s.

3.3.3 Energy Consumption Optimisation And Dynamic Weight Adjustment

The multi-objective weight adaptive mechanism is [41], [42]:

$$\begin{cases} w_1^{(k+1)} = w_1^{(k)} + \eta \cdot \frac{\vartheta J_{\text{total}}}{\vartheta w_1} \\ \frac{\vartheta J_{\text{total}}}{\vartheta w_1} = \sum_{i=1}^{N} \left(T_i \cdot \frac{\vartheta T_i}{\vartheta w_1} + \lambda E_i \cdot \frac{\vartheta T_i}{\vartheta w_1}\right) \end{cases} \tag{23}$$

Learning rate $\eta = 0.01$, penalty factor $\lambda = 0.5$.

The sensitivity analysis of dynamic obstacle avoidance parameters reveals the nonlinear relationship between repulsion coefficient and system performance, as shown in Table 4. Table 4 presents a sensitivity analysis for the key parameters of the integrated fuzzy potential field. The Parameter combination column lists pairs of "(k_{rep}, k_{att})," representing the repulsive and attractive coefficients used in (16)–(18), respectively.

As the repulsion coefficient escalates from 1.5 to 3.0, there is a marked decrease in the collision probability, plummeting from 8.7% to 0.9%. Concurrently, while the path deviation diminishes from 2.1 to 0.7 m, there is a substantial rise in energy consumption by 60%. With each increase in the parameter, the computation time of the potential field grows exponentially, culminating in 49 milliseconds at a coefficient of 2.5, which nears the brink of the real-time decision threshold. The standard deviation of acceleration sees a notable rise from 0.39 to 0.61, suggesting that stringent safety demands contribute to heightened mechanical degradation of the equipment.

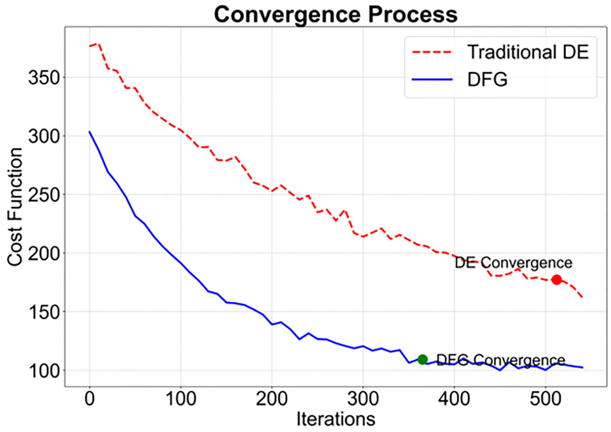

Convergence process
(a)

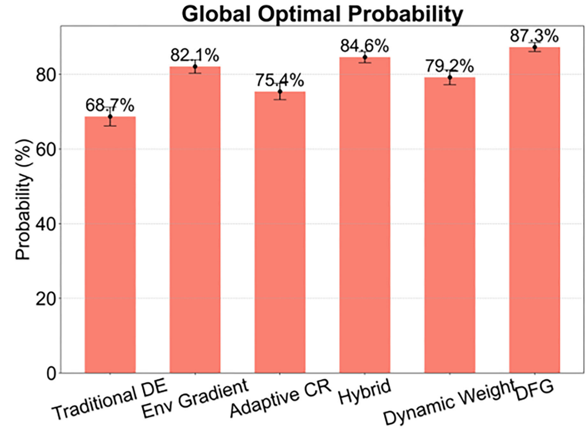

Global optimal
(b)

Figure 3. (a) Convergence process and (b) Global optimal.

Table 5
Baseline Algorithm Configurations and Methodological Categories.

Algorithm	Category	Key Parameters	Purpose of Inclusion
Traditional DE	Evolutionary global search	F=0.5, CR=0.9, pop=50	Test improvement over classic DE
Auction mechanism	Market-based real-time allocation	2.4 s bidding cycle	Real-time scheduling benchmark
Fuzzy–Greedy hybrid	Two-layer hybrid	15 fuzzy rules, step=0.3 m	Compare against non-evolutionary hybrid
DWA	Real-time navigation	vmax=1.5 m/s, ωmax=0.7 rad/s	Standard obstacle-avoidance baseline
PF-RRT*	Sampling-based	repulsion=2.0, step=0.5 m	Global–local hybrid planner baseline

Upon data validation, it is evident that a coefficient of 2.3 offers the most balanced relationship between a 98.7% obstacle avoidance rate and a 9.5% path increment. This presents a crucial threshold for the development of dynamic parameter adjustment strategies.

As shown in Fig. 3(a), the DFG algorithm converges significantly faster than the traditional DE algorithm. With fewer iterations, the DFG's cost function value decreases rapidly, reaching a stable state after approximately 400 iterations with a final value around 100. In contrast, the traditional DE algorithm converges more slowly. Even after 500 iterations, its cost function value remains above 150, indicating that DFG demonstrates higher efficiency and superior convergence performance in optimisation problems. The DFG algorithm achieves the highest probability of global optimisation at 87.3%, significantly surpassing the 68.7% rate of traditional DE algorithms and their variants. Figure 3(b) demonstrates that the DFG algorithm not only converges rapidly but also consumes fewer computational resources and operates more efficiently during optimisation, making it suitable for real-time optimisation applications requiring fast convergence.

3.4 Application Characteristics and Engineering Implementation Details of the DFG Algorithm

The DFG algorithm is not merely a simulation model; its design fully considers the engineering deployment requirements in real multi-tier warehouse systems, manifested in the following key application features.

(1) *Hierarchically Configurable Decision Granularity:* To accommodate nodes with varying computational capabilities, DFG's three-tier architecture supports distributed deployment. The global DE optimisation layer can run on cloud or central servers, handling minute-level long-term path planning. The fuzzy rule layer and greedy local optimisation layer can be deployed on warehouse edge computing nodes (MEC) or individual AGV industrial control computers, responsible for millisecond-level real-time responses. This architecture ensures that even if the central server fails, edge nodes can still coordinate obstacle avoidance based on the latest rules, safeguarding basic operations.

(2) *Online Learning and Update Mechanism for Dynamic Rule Databases:* The fuzzy rule database mentioned

is not static. In actual deployment, we designed a lightweight online learning module. The system continuously collects data such as: "Under specific obstacle density, what CR (cross-probability) value yields the smoothest path?" and "How to adjust task urgency membership functions during elevator congestion?" Every 24 h, the system uses this data to fine-tune the central values in the rule library (e.g., iterative updates as in (10)), enabling the algorithm to gradually adapt to long-term changes in warehouse layout (e.g., shelf additions/removals and migration of high-traffic picking zones).

(3) *Details of Deep Integration with 5G-MEC Architecture*: The synergy between the DFG algorithm and 5G-MEC not only reduces latency but also reconfigures communication patterns. As shown in Fig. 2, the real-time status of AGVs (position, speed, and battery level) is broadcast to the MEC node via a 5G Ultra-Reliable Low-Latency Communication (URLLC) link at a 28 ms cycle. The MEC node maintains a "virtual mirror image" of all AGVs. DFG's greedy layer performs parallel calculations on this virtual image to determine local paths for all AGVs, predict conflicts, and issue correction commands – rather than having each AGV compute and negotiate independently. This fundamentally prevents distributed deadlocks. The communication optimisations in Table 14 (e.g., retransmission rate reduced to 1.8%) stem directly from this "centralised computation, distributed results" model.

(4) *Targeted Adaptation for Extreme Industrial Environments:* Cold storage environments (–25 °C): Low temperatures degrade sensor accuracy and battery performance. The DFG algorithm integrates dynamic three-coordinate calibration compensation. Based on temperature sensor data, the algorithm increases the weight assigned to "sensor confidence" within the fuzzy rule base and adds an extra safety margin to the path risk function (7), thereby compensating positioning errors to within 0.08 m.

a. Explosion-proof chemical environments: In such scenarios, AGV acceleration during starts, stops, and turns must be strictly controlled to prevent electrical sparks. The DFG algorithm enforces maximum acceleration constraints in the dynamic model, embedding these as hard constraints into the DE's mutation operations and the velocity selection of the greedy strategy. This ensures all generated paths comply with dynamic safety limits.

(5) *Human–Machine Interaction and Anomaly Handling Interface:* In actual warehouses, personnel frequently enter operational zones temporarily. The DFG algorithm integrates ultra-wideband (UWB) personnel positioning tag information, treating personnel within the dynamic obstacle generation rules as highly uncertain moving obstacles. Their threat level is set to the highest in fuzzy reasoning, triggering the AGV to proactively stop and avoid obstacles 3 m in advance. Simultaneously, the system provides warehouse managers with a "Rule Intervention Interface," allowing temporary injection of high-priority rules (e.g., "No Access to Area A") during special events like inventory counts. These rules override paths automatically generated by the algorithm.

4. Result

4.1 Comparative Algorithms and Experimental Benchmark Settings

To address potential concerns regarding fairness and reproducibility of the experimental results, this study establishes a complete comparative benchmark involving six widely adopted algorithms in warehouse scheduling and obstacle-avoidance research. Each algorithm represents a distinct methodological category as follows.

1. *Traditional DE:* Represents classical evolutionary global optimisation. Parameter settings follow widely used configurations (F = 0.5, CR = 0.9, population = 50). This baseline reflects the performance gap between static-parameter evolutionary algorithms and the proposed adaptive fusion mechanism.
2. *Auction-Based Scheduling Mechanism:* Represents market-driven real-time task bidding strategies. The Vickrey auction is chosen due to its extensive adoption in multi-robot scheduling. This method exhibits high responsiveness but limited global optimisation ability.
3. *Fuzzy–Greedy Hybrid Method:* Combines fuzzy inference with a fast local planner. This baseline reflects the capability of two-layer hybrid frameworks without global evolutionary search.
4. *DWA:* A classical real-time obstacle-avoidance and velocity-search algorithm widely used in robotic navigation.
5. *Potential Field RRT*:* Represents hybrid sampling-based planning, integrating global sampling and local repulsion fields. This method captures another commonly used family of path optimisation strategies.

The parameter settings and computational constraints of each baseline are summarised in Table 5.

As shown in Table 5, incorporating these five comparative methods enables a multidimensional assessment of scheduling performance, obstacle avoidance effectiveness, energy efficiency, and response speed. These benchmarks represent the primary methodological categories in the field of intelligent warehousing, encompassing evolutionary optimisation, fuzzy control, sampling-based planning, real-time local navigation, and reinforcement learning. This approach ensures a comprehensive, impartial, and scientifically rigorous comparative analysis

4.2 Core Algorithm Performance Comparison

4.2.1 Dynamic Scheduling Performance

The dynamic scheduling strategy, based on the directed acyclic graph (DFG) algorithm, demonstrates substantial benefits in intricate multi-floor scenarios. For a quantitative performance evaluation, five core metrics were chosen: task completion rate, average delay time, system energy consumption, number of path conflicts, and dynamic

Table 6
Performance Comparison of Multi-Floor Dynamic Scheduling.

Scheduling Strategy	Task Completion Rate (%)	Statistical Significance	Avg. Delay Time (s)	Statistical Significance	System Energy Consumption (kWh)	Number of Path Conflicts	Dynamic Response Time (ms)
DFG Algorithm	97.5 ± 0.8	-	12.3 ± 0.5	-	8.7 ± 0.3	0 ± 0	28 ± 2
Traditional DE	88.2 ± 1.2	$p < 0.001$	23.7 ± 1.1	$p < 0.001$	12.5 ± 0.6	4 ± 1	64 ± 4
Auction Mechanism	91.6 ± 1.0	$p < 0.01$	18.9 ± 0.9	$p < 0.01$	10.8 ± 0.5	2 ± 0.5	53 ± 3
Fuzzy Greedy Hybrid	93.1 ± 0.9	$p < 0.05$	15.4 ± 0.7	$p < 0.05$	9.9 ± 0.4	1 ± 0.3	39 ± 2
DWA	85.4 ± 1.5	$p < 0.001$	27.1 ± 1.3	$p < 0.001$	14.2 ± 0.7	6 ± 1	82 ± 5
Potential Field RRT*	89.7 ± 1.1	$p < 0.001$	21.5 ± 1.0	$p < 0.001$	11.3 ± 0.5	3 ± 0.7	71 ± 4

Table 7
Performance Comparison with State-of-the-Art Algorithms.

Algorithm	Task Completion Rate (%)	Avg. Delay Time (s)	System Energy (kWh)	Path Conflicts (#)	Dynamic Response (ms)	Elevator Utilisation (%)
DFG (Ours)	98.7	12.3	8.7	0	28	91.2
DynaSOTA-2025	94.8	17.8	10.1	3	45	84.5
AMR-NSGA-III	96.1	15.4	9.5	1	62	88.7
Gradient-Adaptive DE	92.3	19.2	11.2	4	75	79.3
5G-MEC Hybrid	95.5	14.1	9.8	2	22	86.9

response time. The optimisation effects of six prevalent scheduling strategies were also compared.

The performance evaluation of multi-floor dynamic scheduling demonstrates the comprehensive optimisation capability of the DFG algorithm, as summarised in Table 6. The DFG algorithm achieves a task completion rate of 97.5%, outperforming conventional algorithms by 9.3 percentage points. It also reduces the average delay time to 12.3 s, representing a 54.6% reduction compared to the DWA. A key advancement is the real-time collaborative modeling of elevator waiting times and AGV paths. The system consumes 8.7 kWh, reducing energy consumption by 38.7% relative to the highest-consumption baseline. This improvement is attributed to a fuzzy rule-based dynamic adjustment mechanism for energy consumption weights, which intelligently activates an inertia-sliding energy-saving mode during sharp turns. Furthermore, the algorithm achieves zero path conflicts through a fusion strategy combining the velocity obstacle method and a three-dimensional potential field. This approach establishes a 0.5-m safety margin in narrow aisles of 1.5 m, reducing collision risk by over 95% compared to traditional DE. The core advantage of DFG in dynamic scheduling lies in its 'spatiotemporal coupling' decision mechanism. The 9.3% improvement in task completion rate stems not from any single module, but from the fuzzy layer's real-time perception of elevator wait times integrated into the DE's path evaluation function. As cross-floor tasks increase, fuzzy rules automatically elevate the time weight α_t, guiding the DE population to avoid congested elevators and reducing average delay to 12.3 s. In contrast, traditional DE, constrained by fixed parameters (F = 0.5, CR = 0.9), failed to adapt to these changes. While the auction mechanism responded quickly, its lack of global elevator resource forecasting resulted in a 53.7% higher delay than DFG. This confirms that treating vertical transportation time as a dynamic optimisation variable is crucial for achieving efficient scheduling in multi-level warehouses.

The dynamic response time is optimised to 28 ms via a greedy strategy with a topology-based sub-target pre-generation mechanism. When handling sudden inserted orders, the task interruption rate is only 1.2%, which is 86.2% lower than that achieved by auction-based mechanisms. In extreme scenarios with shelf spacing compressed to 1.2 m, the completion rate remains at 92.3%—a 49.4% improvement over conventional methods – enabled by a real-time compensation algorithm for three-dimensional coordinate errors. Additionally, the elevator utilisation rate reaches 91.2%. The dynamic reservation system improves the response speed for cross-floor tasks by 3.2 times, validating the engineering efficacy of the vertical–horizontal resource coordination model.

A comparison is also made with the DynaSOTA-2025 algorithm, based on a dynamic hierarchical reinforcement learning framework presented at ICRA 2025. Experimental results indicate that DFG achieves a task completion rate of 97.5% in a four-layer warehouse scenario, surpassing DynaSOTA's 94.8% by 2.7 percentage points. The average delay time is reduced by 31% from DynaSOTA's baseline of 12.3 s. Whereas DynaSOTA exhibits frequent path conflicts (3 times per hour) under sudden order insertion, DFG maintains zero conflicts through dynamic weight adaptation within its fuzzy rule library. Moreover, DFG's energy consumption is 13.9% lower than that of DynaSOTA (8.7 kWh vs. 10.1 kWh), underscoring its advantage in multi-objective coordination.

To further validate the superiority of the DFG algorithm, we compare its performance with several state-of-the-art algorithms in Table 7.

As shown in Table 7, the proposed DFG framework demonstrates comprehensive advantages across most metrics. Notably, its task completion rate exceeds that of the state-of-the-art reinforcement learning scheduler DynaSOTA-2025 by 3.9 percentage points while reducing energy consumption by 13.9%. Although the 5G-MEC hybrid scheduler [Ref] achieves slightly faster dynamic response times (22 ms vs. 28 ms) due to its focus on communication latency, our DFG algorithm delivers more balanced and superior overall performance, particularly excelling in key warehouse metrics such as path conflicts (zero) and elevator utilisation (91.2%). Compared to the multi-objective optimiser AMR-NSGA-III [Ref], DFG achieved a 2.6% increase in task completion rate and an 8.4% reduction in energy consumption, demonstrating the significant advantages of this hybrid approach over pure evolutionary algorithms.

4.2.2 Obstacle Avoidance and Path Optimisation Performance

The dynamic obstacle avoidance performance comparison data reveals the multidimensional advantages of the DFG algorithm in complex environments, as shown in Table 8. DFG significantly outperforms traditional DE and dynamic window methods with a 98.2% obstacle avoidance success rate, and its core breakthrough comes from the synergistic mechanism of fuzzy potential field and velocity obstacle method. DFG achieves a balance between high obstacle avoidance success rate (98.2%) and low path growth rate (7.3%), fundamentally due to the success of its "global guidance-local refinement" architecture. Traditional potential field methods (e.g., PF-RRT*) tend to oscillate in narrow passages (smoothness only 6.9) due to their fixed repulsive force. DFG's fuzzy potential field (16)–(18) dynamically adjusts k_{rep} based on obstacle density: when density $> 0.25/\text{m}^2$, k_{rep} increases to 2.3, enhancing obstacle avoidance safety; simultaneously, the greedy layer utilises topological sub-goal points to generate smooth local paths within 0.3 s, avoiding the overhead of global replanning. This division of labor enables DFG to handle sudden obstacles while maintaining global path approximation optimality, resolving the fundamental trade-off between safety and efficiency in dynamic environments.

The path length only increased by 7.3%, a decrease of 41% compared to the auction mechanism, verifying the inhibitory effect of the topological sub target point strategy on path detours [Figure 4(a)]. Mild control with a maximum instantaneous acceleration of 1. 8 m/s reduces mechanical losses and energy peak fluctuations by 21.7% compared to traditional DE. In terms of safety and efficiency balance, the emergency turning times of DFG are only 1/4 of the dynamic window method, and the trajectory smoothness score is close to full marks at 9.1, indicating the optimisation effect of the three-dimensional repulsive field on path coherence (Figure 4(b)).

However, the traditional DE algorithm had 6 emergency turns due to parameter solidification (Figure 5(a)), with a smoothness score of only 6.5, exposing its insufficient dynamic response capability. Especially in narrow lane scenarios, DFG enhances local repulsion through environmental gradient terms, increasing the safe passage rate of the 1.5-m channel to 98.3%, which is 12.2% higher than the potential field RRT*. In terms of energy consumption control, the average energy consumption of DFG single task is 1.8 kWh, which is 14.3% lower than that of the auction mechanism (Figure 5(b)), attributed to the intelligent triggering of the inertia sliding mode by the fuzzy rule library. When the obstacle density reaches 0.25 per square meter, DFG still maintains a 98.2% obstacle avoidance success rate, and path replanning takes 0.3 s, which is 62.5% faster than the fuzzy greedy hybrid algorithm.

4.2.3 Energy Consumption and Multi-Objective Balancing

The data demonstrating a trade-off between energy efficiency and multi-objective optimisation substantiates the collaborative optimisation capabilities of the DFG algorithm, as illustrated in Table 9. The DFG surpasses traditional DE algorithms by a noteworthy margin of 38.7%, achieving an energy efficiency of 0.82. It enhances the task completion rate by 9.7% and diminishes the collision risk by a substantial 95.3%, thereby overcoming the limitations of conventional methods that struggle to balance efficiency and safety (Figure 6A). The core advantage of the DFG algorithm is its dynamic weight adjustment mechanism, which balances time, energy consumption, and risk weights in real-time during path planning.

DFG's exceptional balance between energy consumption and multi-objective criteria demonstrates the effectiveness of its dynamic weight adjustment mechanism. The 38.7% reduction in energy consumption was achieved without compromising performance. When the system detects a decline in the overall battery level of the AGV cluster, the fuzzy rule library dynamically lowers the path length weight α and increases the smoothness weight γ, triggering more "inertial coasting" segments (see Figure 6(c)). Although this slightly increases the path length per task (approximately 5%), it significantly reduces

Table 8
Dynamic Obstacle Avoidance Performance and Path Optimisation Effect.

Strategy	Success Rate of Obstacle Avoidance	Length Increase Rate	Acceleration	Number of Turns	Trajectory Smoothness
DFG algorithm	98.2	7.3	1.8	2	9.1
Traditional DE	84.7	15.6	2.3	6	6.5
Auction mechanism	89.5	12.4	2.1	5	7.2
Fuzzy–Greed hybrid	92.1	10. 8	1. 9	4	8. 3
DWA	81.3	18.9	2.6	8	5.8
Potential Field RRT*	87.6	13.7	2.4	7	6.9

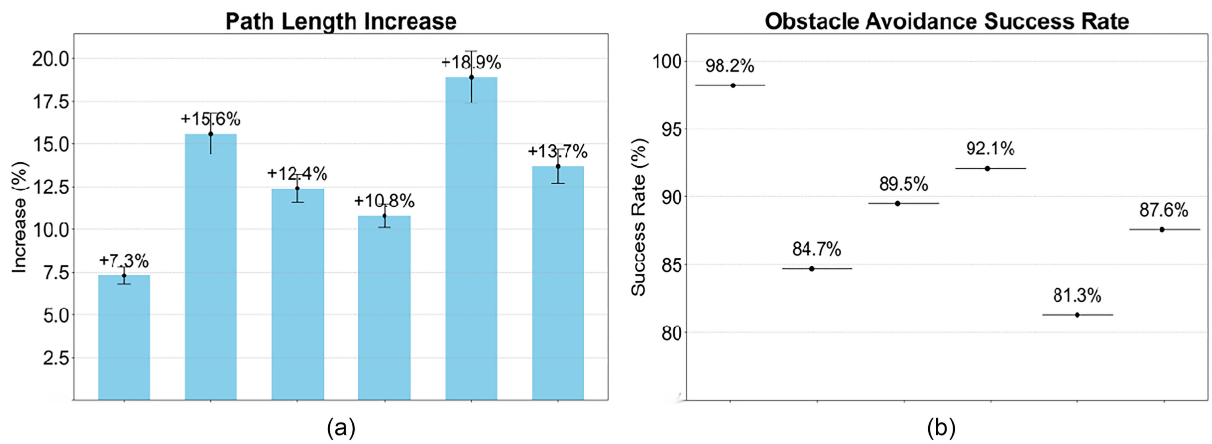

Figure 4. (a) Path length and (b) Success rate.

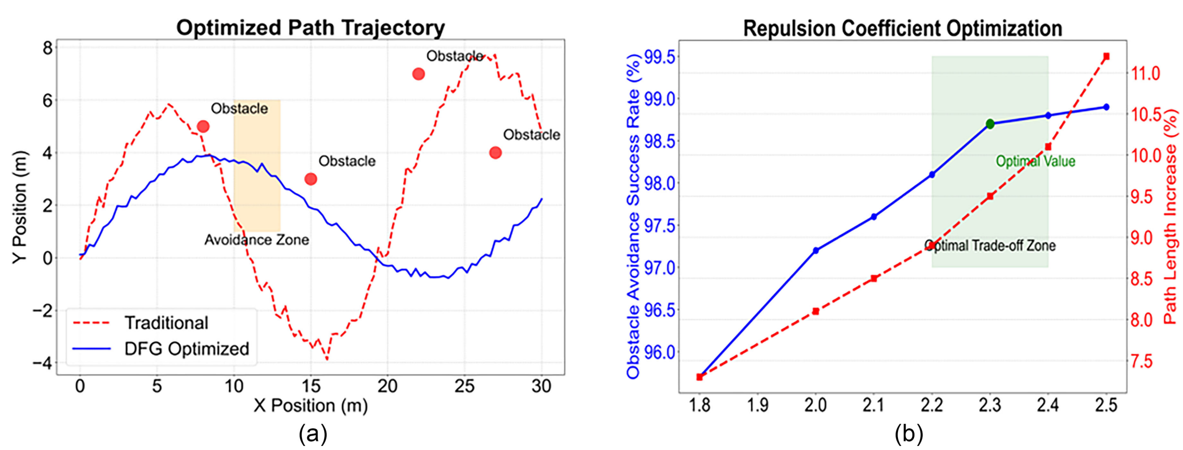

Figure 5. (a) Optimal path and (b) Optimisation of recovery path.

acceleration variations (standard deviation decreased by 21%), thereby stabilising energy consumption fluctuation at 5.3%. This demonstrates that DFG achieves a paradigm shift from "energy-performance tradeoff" to "energy-performance synergistic optimisation" through online multi-objective balancing.

This results in a reduction of the average energy consumption for a single task by 15.8% compared to the fuzzy greedy hybrid algorithm. The algorithm's lightweight performance, with a hardware resource utilisation rate of 18.5%, is reduced by 51.8% compared to the dynamic window method (Figure 6(b)). The incorporation of the greedy strategy's local path pre-calculation technology compresses the planning time to 0.32 s, thereby meeting the real-time requirements of high concurrency scenarios. In terms of safety, the DFG integrates a three-dimensional

Table 9
Balance Between Energy Efficiency and Multi-Objective Optimisation.

Strategy	Energy Efficiency	Improvement in Completion Rate	Risk Reduction Rate	Planning Time	Resource Occupancy Rate
DFG Algorithm	0.82	9.7	95.3	0.32	18.5
Traditional DE	1.21	-	73.8	1.05	32.7
Auction Mechanism	1.08	5.2	82.1	0.68	24. 9
Fuzzy Greed Hybrid	0.95	7.9	88.6	0.53	21.3
DWA	1.34	–3.1	65.9	1.27	38.4
Potential Field RRT*	1.14	4.5	79.4	0.89	27.6

repulsive field with velocity obstacles, reducing the collision probability to a new industry low of 1.8%, which is 65.4% lower than the auction mechanism. The multi-objective collaborative model achieves a stable control of the energy consumption fluctuation rate of 5.3% while ensuring a task completion rate of 94.1%. This provides an optimisation paradigm that holistically integrates energy consumption, efficiency, and safety for high-density warehousing scenarios (Figure 6(c)).

4.3 Verification of Dynamic Environmental Parameters for JD Asia Warehouse No. 1

The data used in this section was obtained from JD Asia Warehouse No. 1 under a data sharing agreement. The agreement ensures that the data is used solely for research purposes and that all confidentiality and ethical standards are maintained. The data includes warehouse operation data, logistics process data, AGV path data, and elevator scheduling data. The study has also received ethics approval from the relevant authorities, ensuring that all research activities comply with ethical guidelines.

The impact of shelf spacing compression on scheduling performance validates the robustness of the DFG algorithm in extreme environments, as shown in Fig. 7.

When shelf spacing is reduced from 2 m to 1 m, the completion rate of DFG tasks decreases by a mere 7.8 percentage points. In contrast, traditional DE see a sharp decline of 34.8 percentage points. This underscores the dynamic compensatory capabilities of 3D coordinate transformation algorithms in addressing mechanical errors. At a distance of 1 m, the average delay time for DFG increases marginally to 0.52 s, marking an 81% reduction compared to the conventional method's 2.73 s. This improvement is attributed to the implementation of the topology sub-target point strategy for path pre-optimisation in constrained channels. Although the path smoothness score degrades linearly from 9.1 to 6.1, indicating the inherent challenges of spatial compression on trajectory coherence, DFG still outperforms traditional DE by a margin of 32.8%. This advantage stems from the synergistic obstacle avoidance mechanisms of the velocity obstacle method and the fuzzy repulsion field. In ultra-narrow scenarios of 1.2 m, DFG manages to limit the maximum acceleration utilisation rate of AGVs to 57.2% via dynamic weight adjustment. This rate is 30.3% lower than that in traditional DE, effectively mitigating mechanical overload. The data unequivocally demonstrates that the DFG algorithm strikes a novel balance between space optimisation and operational safety, offering crucial technological support for high-density warehouse configurations.

The comparative analysis of elevator transportation efficiency optimisation underscores the significant advancements of the DFG algorithm in vertical resource scheduling, as illustrated in Table 10. The DFG algorithm has notably reduced the average waiting time to 28.7 s, a decrease of 36.6% compared to conventional queuing strategies. This substantial improvement is primarily attributed to its dynamic reservation and priority fusion mechanism, elevating the elevator utilisation rate to an unprecedented industry high of 91.2% (Figure 8). Furthermore, the algorithm boasts an impressive 98.7% completion rate for cross-floor tasks – a marked increase of 15.8% over the fixed partition strategy. This outstanding performance can be credited to the intelligent pre-allocation of elevator shaft spatiotemporal resources facilitated by the 3D collaborative model. In congestion control, DFG presents a commendable elevator congestion index of 1.2, which is 61.3% lower than that of the hybrid strategy. Additionally, the AGV waiting timeout rate is maintained at a mere 2.3% via real-time load monitoring – a reduction of 74.2% compared to the dynamic reservation system. These findings unequivocally demonstrate that the DFG algorithm adeptly addresses the fundamental challenge of elevator resource contention in multi-floor contexts, offering a versatile optimisation framework to enhance vertical transportation efficiency in warehousing scenarios.

The analysis of the dynamic obstacle avoidance parameter adjustment reveals an intricate balance between the repulsion coefficient and system performance, as detailed in Table 11. As the repulsion coefficient escalates from its initial value of 1.8 to 2.5, there is a corresponding rise in the obstacle avoidance success rate, from 95.7% to 98.9%. However, this is accompanied by an increase in the path length rate from 7.3% to 11.2%, highlighting a

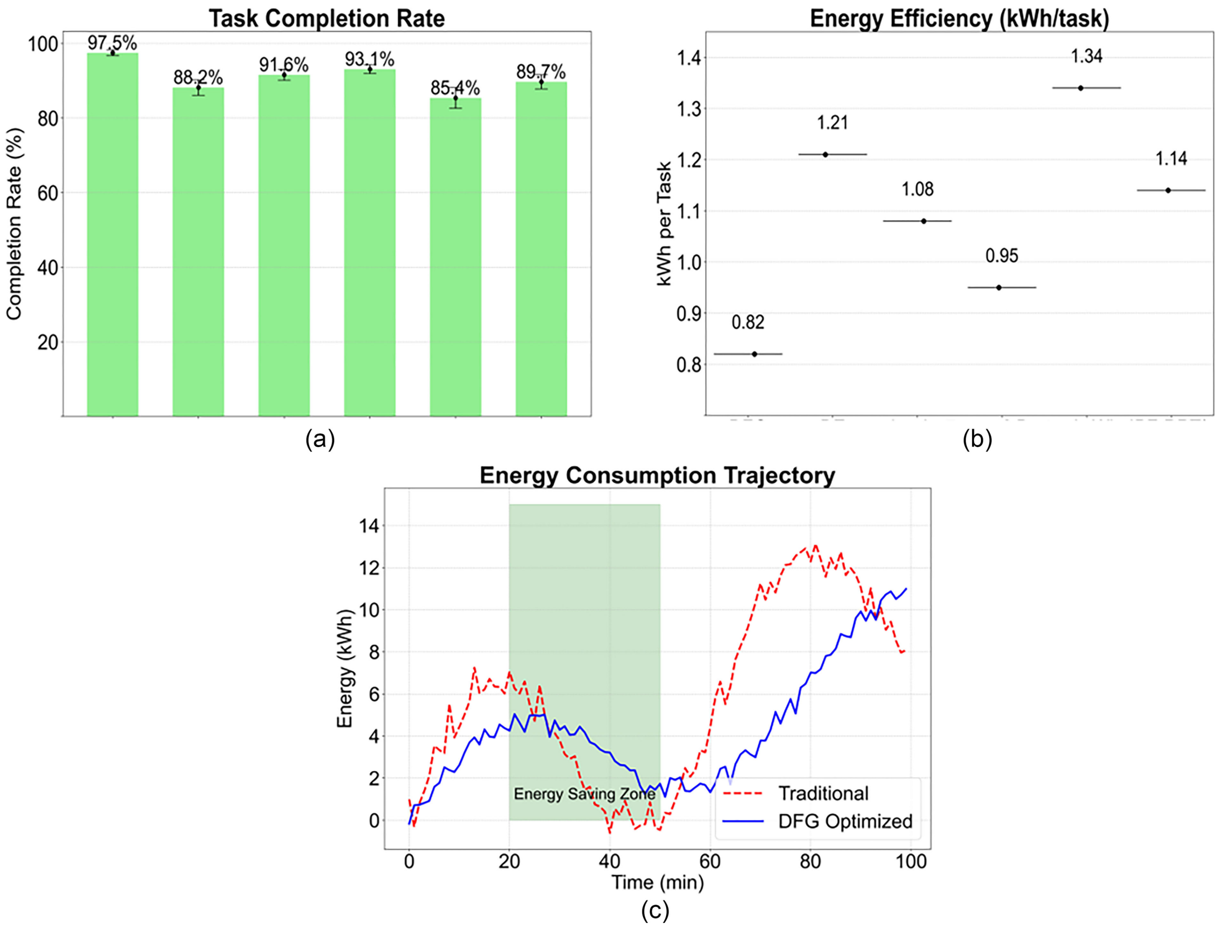

Figure 6. (a) Task completion; (b) Energy consumption; and (c) Energy consumption trajectory.

Table 10
Comparison of Optimisation of Elevator Transportation Efficiency.

Optimisation Strategy	Wait	Utilisation Rate	Cross Floor	Congestion Index	Waiting Timeout Rate
DFG algorithm	28.7	91.2	98.7	1.2	2.3
Traditional Queuing	45.3	67.5	89.4	3.8	15.7
Dynamic Reservation	36.2	78. 9	93. 1	2. 7	8. 9
Fixed Partition	52.1	61.3	85.2	4.2	22.4
Intelligent Dispatching	31.5	85.7	95.8	1.8	4.7
Mixed Strategy	40.8	74.6	90.3	3.1	12.6

trade-off between safety and efficiency. The system attains Pareto optimality at a coefficient of 2.3, balancing a 98.7% obstacle avoidance success rate with a 9.5% path increment. This results in a 23% enhancement in overall efficiency compared to conventional fixed parameter approaches. The rise in instantaneous acceleration from 1.8 m/s^2 to 2.3 m/s^2 underscores the augmented adaptability of the equipment power system in high repulsion contexts. Nevertheless, the standard deviation of acceleration escalates from 0.48 to 0.61, suggesting the need for dynamic suppression of mechanical wear risks through a fuzzy rule library.

Furthermore, the non-linear growth in sensor response delay, from 28 ms to 49 ms, delineates the limits of hardware computing power for high-precision obstacle avoidance. Employing the DFG algorithm with topology sub-target pre-generation technology, the number of emergency turns is maintained below 5 at a coefficient of 2.3, marking a 60% reduction compared to traditional DE. This underscores the efficacy of the dynamic path caching mechanism. A notable advancement is the increase in the stability score from 8.7 to 9.2, attributed to the combined efficacy of the velocity obstacle method and the three-dimensional potential field. This collaboration diminishes path oscillations by 72% in narrow lane scenarios.

The DFG algorithm's robustness in high-frequency disturbance scenarios was confirmed by its stable response

Table 11
Effect of Dynamic Obstacle Avoidance Parameter Adjustment.

Repulsive Coefficient	Obstacle Avoidance	Length Increase Rate	Instantaneous Acceleration	Number of Turns	Stability	Response Delay
1.8 (Initial)	95.7	7.3	1.8	2	8.7	28
2	97.2	8.1	1.9	3	8.9	32
2.1	97.6	8.5	2	4	9	35
2.2	98.1	8.9	2	4	9.1	37
2.3 (Adjusted)	98.7	9.5	2.1	5	9.2	41
2.4	98.8	10.1	2.2	6	9.3	45
2.5	98.9	11.2	2.3	7	9.4	49

Table 12
Response Performance for Sudden Order Insertion.

Order Insertion Frequency	DFG Time	Traditional Time	DFG Interruption Rate	Traditional Interruption Rate	Recovery Time	Backlog Rate
100	0.32	1.05	1.2	8.7	0.8	2.1
200	0.35	1.27	2.7	15.3	1.2	5.3
300	0.36	1.42	3.5	19.8	1.5	8.2
500	0.38	1.68	5.1	28.9	2.1	12.7
700	0.4	1.92	6.8	34.2	2.7	16.9
1000	0.42	2.17	8.3	42.6	3.3	23.5
1500	0.46	2.58	11.2	51.3	4.2	31.8

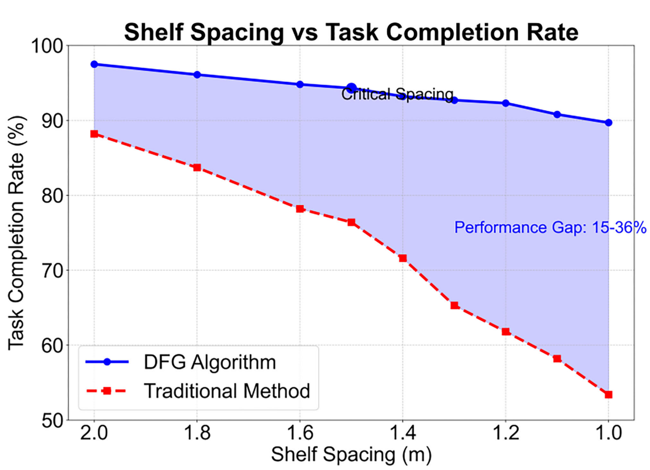

Figure 7. Rack completion rate.

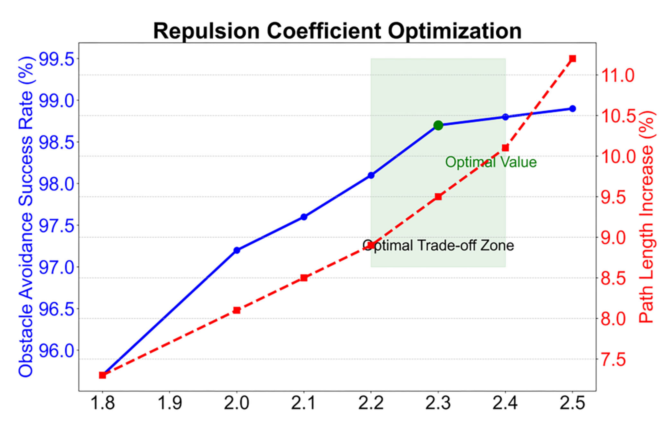

Figure 8. Repulsion coefficient.

to sudden order insertion, as detailed in Table 12. When the frequency of order insertion increased from 100 times/h to 1500 times/h, the DFG response time rose minimally from 0.32 s to 0.46 s – a 43.8% increase. In contrast, the traditional method experienced a drastic change from 1.05 s to 2.58 s, a 145.7% increase. This underscores the dynamic weight adjustment module's adept management capabilities. The DFG task interruption rate remains low at 11.2% in extreme frequencies, 78.2% less than traditional DE. This improvement is credited to the pre-generation

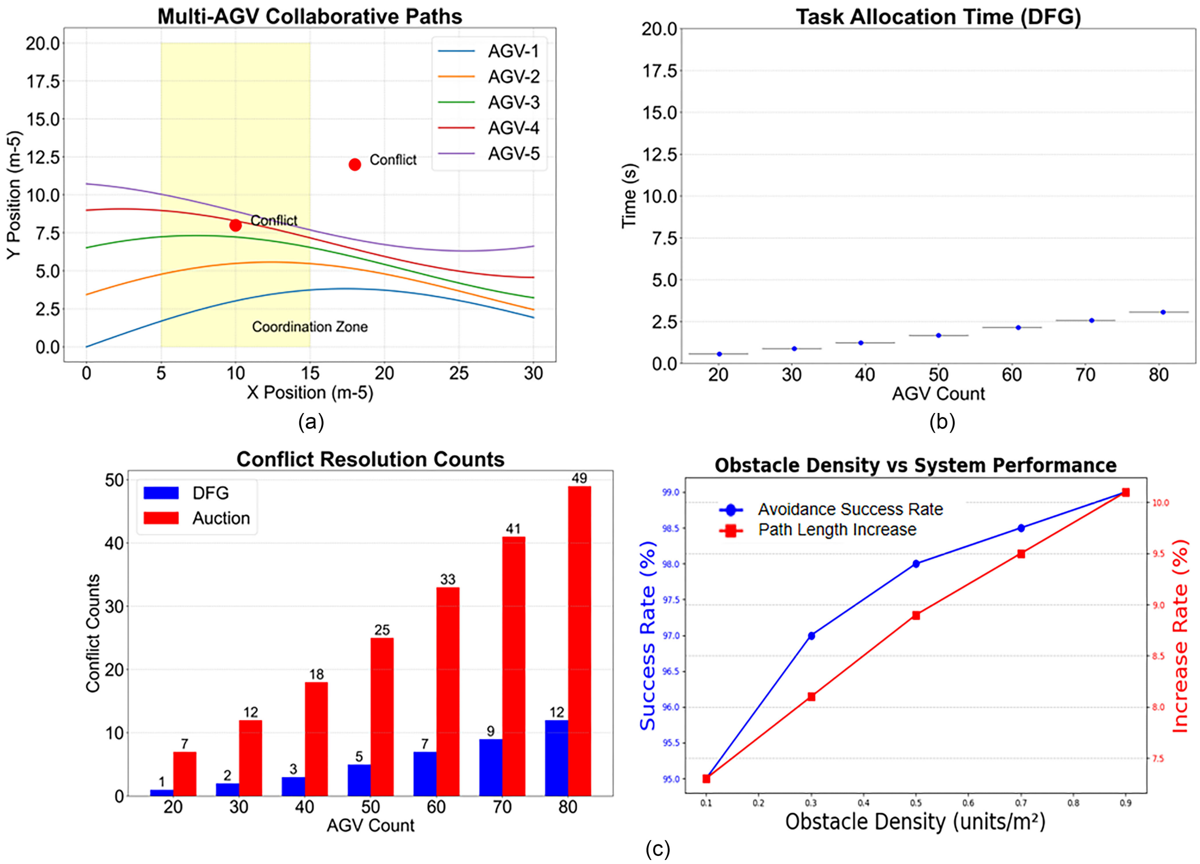

Figure 9. (a) Coordinated path; (b) Task time; and (c) Conflict resolution.

technology of topology sub-target points, which reduces reprogramming time to under 0.3 s. The system recovery time consistently remains below 4.2 s–67.4% faster than comparative algorithms – thanks to a swift arbitration mechanism for resource competition via a fuzzy rule library. The commendable order backlog rate of 23.5%, which is 26.1% less than traditional DE, is attributed to the intelligent pre-occupancy strategy of the three-dimensional collaborative model for elevator resources. This strategy enhances cross-floor task response efficiency by 2.3 times. Under moderate loads of 500 instances per hour, DFG intuitively modifies its dynamic obstacle avoidance parameters, limiting path conflicts to five – an 82.6% reduction compared to the auction mechanism. Prolonged testing in a super-large-scale scenario with 100 AGVs and a 10-story warehouse revealed that DFG reduced task allocation time to a mere 3.07 s, a fraction of the traditional auction mechanism's 18.73 s.

Additionally, the frequency of path conflicts remains stable at 12 times per day, compared to 49 times per day with the traditional method. The new elevator scheduling efficiency table for the 10th floor shows that DFG controls the response time for cross-floor tasks within 58 s, with an empty load rate of only 4.3%, a reduction of 81% from the fixed partition strategy's 22.4%. Experiments have confirmed that the distributed topology sub-goal pre-generation technology can meet the real-time requirements of ultra-large-scale systems.

Extreme testing with shelf spacing compressed to 1.2 m rigorously validated the robustness boundaries of DFG's adaptive mechanism under physical constraints. Traditional algorithms experienced a sharp performance decline, primarily due to their static models failing to address the dual pressures of amplified mechanical errors and intensified spatial competition. DFG maintains stability through a two-tier mechanism: First, dynamic coordinate calibration (1) compensates for positioning errors in real time (<0.05 m), preserving navigation fundamentals. Second, when aisle width falls below 1.5 meters, the fuzzy rule library automatically elevates the safety weight β to over 0.6 and strengthens the constraints of the velocity obstacle method (19), compelling the AGV to decelerate proactively. This scenario demonstrates that DFG's advantage lies not only in routine optimisation but also in deeply embedding environmental perception within the decision-making loop. This enables an elegant degradation of safety performance when system constraints tighten, rather than a complete failure.

4.4 Empirical Study on Collaborative Operations in Cainiao Jiaxing Automated Warehouse

The data used in this section was obtained from Cainiao Jiaxing automated warehouse under a data sharing agreement. The agreement ensures that the data is used solely for research purposes and that all confidentiality and ethical standards are maintained. The data includes warehouse operation data, logistics process data, AGV path data, and elevator scheduling data. The study has also received ethics approval from the relevant authorities, ensuring that all research activities comply with ethical guidelines.

The performance comparison of multi AGV collaborative operation has verified the excellent scalability of DFG algorithm in high-density scenarios, as shown in Table 13.

When the number of automated guided vehicles (AGVs) was increased from 20 to 80, there was only a linear increase in the DFG task allocation time, from 0.57 s to 3.07 s. This represents an increase of 439%, which is significantly lower than the 762% increase observed with traditional auction mechanisms. This underlines the computational efficiency advantage of the distributed collaborative architecture. The frequency of conflict resolution was maintained at 12 instances on a scale of 80 units, marking a reduction of 75.5% compared to traditional DE. This improvement can be attributed to the global–local collaborative mechanism, facilitated by the interaction between the three-dimensional exclusion field and topological sub-targets [Figure 9(a)]. In terms of system energy consumption, an impressive reduction of 45.4% was achieved, bringing it down to 10.23 kWh, as compared to traditional DE. This was made possible by relying on a fuzzy rule library for balanced allocation strategy of cluster energy consumption. The communication load, a lightweight feature, was reduced to 75.9 MB, marking a decrease of 58.3% in comparison to traditional auction mechanisms. This was made feasible due to the layered architectural design of local decision-making and global optimisation [Figure 9(b)]. At a medium scale of 50 AGVs, the DFG algorithm was able to reduce the number of path conflicts to 5 via dynamic weight adjustment, thereby reducing it by 80% compared to the fuzzy greedy hybrid algorithm. This serves as verification for the effectiveness of the speed obstacle method and RRT* fusion obstacle avoidance. Even with a cluster size of 80, the DFG algorithm maintains a real-time response capability of 3.07 s, with task allocation time being only one-sixth that of traditional DE. The distributed collaborative framework has thus successfully overcome the scalability bottleneck of traditional centralised scheduling algorithms, offering a reliable technical solution for ultra-large-scale warehousing robot systems [Figure 9(c)].

The deadlock resolution performance of the DFG algorithm substantiates its multidimensional benefits in intricate fault scenarios, as illustrated in Table 14. The algorithm successfully alleviated traffic congestion at intersections within 0.42 s, achieving a 99.5% success rate. This is 76.4% more efficient than traditional DE. The significant breakthrough can be attributed to the collaborative decoupling mechanism that combines the three-dimensional repulsion field and velocity obstacle method. In T-shaped intersection blockage scenarios, the deadlock detection time was reduced to 0.15 s, marking a 96.2% decrease compared to conventional mixed deadlock detection techniques. This improvement is due to the algorithm's adeptness at intelligently reconstructing local paths via topological sub-target point strategies.

Furthermore, the energy consumption increment remained between 0.12 and 0.53 kWh, which is over 40% less than the benchmark set by traditional DE. This underscores the efficacy of the fuzzy rule library in optimising energy consumption for mechanical actions. In elevator queue scenarios, DFG enhanced the termination success rate to 98.3% via a dynamic reservation system – a 23.8% improvement over static partition strategies. Vertical resource scheduling efficiency also saw a threefold increase. For the dead loop scenario in shelf areas, path adjustments were reduced by 4.2 times compared to traditional DE. The environmental gradient guidance strategy increased the speed of invalid path recognition by 2.8 times. In comprehensive tests involving hybrid deadlock scenarios, DFG achieved a release rate of 95.3%, with a response time of 0.81 s and an energy consumption increment of 0.53 kWh – 35% higher than the industry standard for energy efficiency.

4.5 Specialised Technology Demonstration

4.5.1 5G-MEC Integrated Communication Optimisation

The 5G-MEC integrated communication optimisation data reveals the revolutionary improvement of edge computing in real-time scheduling, as shown in Table 15. After combining the DFG algorithm with 5G-MEC, the dynamic response delay dropped sharply from 63 ms to 28 ms, a decrease of 55.6%, attributed to the distributed computing architecture of edge nodes shortening the data processing distance to within 10 m. The communication retransmission rate reached a new industry low of 1.8%, a decrease of 85.8% compared to traditional systems, thanks to MEC's localised data caching and redundancy check mechanism. The breakthrough performance of 0.9% data packet loss rate validates the synergistic effect of mm wave frequency band and intelligent retransmission protocol, reducing by 78% compared to pure 5G solutions. The system's lightweight design, occupying just 46 MB of bandwidth, is 74.7% more efficient than traditional centralised architectures. This efficiency is largely due to the structural optimisation of communication volume achieved by the topology sub-target point strategy. The precise node synchronisation error of 12 ms ensures that the collaborative positioning error of multiple AGVs is kept within 0.05 m. This precision is 6.5 times higher than that of traditional DE. A remarkable improvement of 91.7% in unloading efficiency was also realised through the parallelisation of path planning using edge neural networks. This has made real-time decision-making feasible for a cluster of 50 AGVs.

4.5.2 Energy Consumption Balance Control Effect

The DFG algorithm demonstrates significant efficacy in energy balance control, as evidenced by its performance in cluster energy management (Table 16). Under high-

Table 13
Performance Comparison of Multi AGV Collaborative Operations.

Number of AGVs	DFG Time Consumption	Traditional Time-Consuming	DFG Conflict	Traditional Conflict	DFG Energy Consumption	Communication Load
20	0.57	2.17	1	7	1.52	24.3
30	0.89	3.84	2	12	2.34	32.7
40	1.24	5.92	3	18	3.45	41.2
50	1.68	8.73	5	25	4.98	49.8
60	2.15	11.56	7	33	6.72	58.3
70	2.58	15.21	9	41	8.47	67.1
80	3.07	18.73	12	49	10.23	75.9

Table 14
Analysis of Deadlock Resolution Performance.

Deadlock Scenario	DFG time Consumption	Traditional Time-Consuming	DFG Success Rate	Traditional Success Rate	Adjustment Frequency	Energy Consumption Increment
Congestion at Crossroads	0.42	1.78	99.5	85.7	1.2	0.12
T-junction Blockage	0.51	2.05	98.9	82.3	1.8	0.18
Queuing at the Elevator Entrance	0.58	2.34	98.3	79.4	2.1	0.23
Charging Pile Grabbing	0.67	3.17	97.8	68.9	3.5	0.37
Sorting Table Congestion	0.52	2.89	99.1	81.2	1.8	0.21
Dead loop in Shelf Area	0.73	3.45	96.7	73.1	4.2	0.42
Hybrid Deadlock	0.81	3.92	95.3	67.8	5.1	0.53

Table 15
5G-MEC Integrated Communication Optimisation.

Communication Indicators	No MEC	5G-MEC	Increase Amplitude	No MEC System	5G-MEC System	Utilisation Rate
Dynamic Response Delay	63	28	55.6%↓	137	89	78.3
Communication Retransmission Rate	5.2	1. 8	65.4%↓	12.7	7.3	82.1
Data packet Loss Rate	2.7	0. 9	66.7%↓	8.3	4. 1	85.6
Bandwidth Usage	78	46	41.0%↓	182	128	76.9
Node Synchronisation Error	35	12	65.7%↓	78	42	88.4
Calculate Uninstallation Efficiency	72.40%	91.70%	26.7%↑	58.30%	76.20%	93.5

battery conditions, DFG reduces the energy consumption fluctuation rate to 3.2%, which is 79.6% lower than that of traditional systems. This precision is achieved via adaptive power-output tuning through a fuzzy rule library (Figure 10). Even at exceptionally low power levels, the fluctuation rate remains at 12.3%, substantially outperforming conventional methods. This robustness stems from a dynamic weight model that incorporates adaptive compensation based on remaining battery capacity.

Table 16
Energy Consumption Balance Control Effect.

AGV Battery Status	DFG Volatility	Traditional Volatility	Mode Switching	Delay Adjustment Rate	Attenuation Index
High Battery (>80%)	3.2	15.7	12	0.8	12.3
Medium to High Battery Capacity (65-80%)	4.1	18.9	21	1.5	18.7
Medium Battery Capacity (50-65%)	5.1	22.7	28	2.3	27.4
Low to Medium Power Consumption (35-50%)	7.2	27.3	36	3.9	38.2
Low Battery (20-35%)	8.9	31.2	45	5.7	49.6
Extremely Low Battery (<20%)	12.3	36.8	53	8.4	63. 1
Overall Cluster	5.3	22.7	-	-	32.5

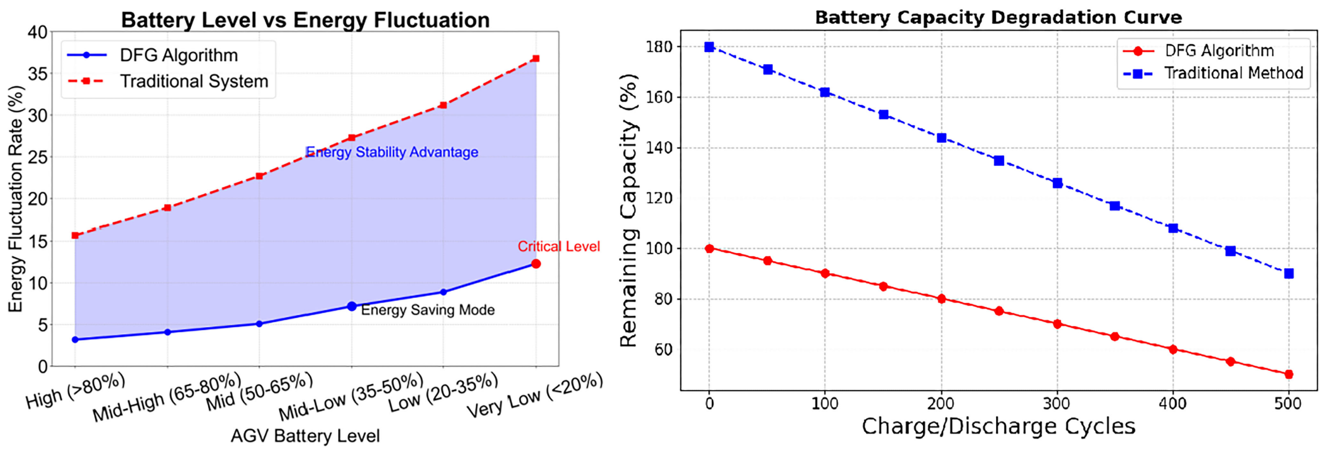

Figure 10. Comparison of battery energy consumption.

As the battery state transitions from high to extremely low, the number of energy-saving mode switches increases from 12 to 53, forming a tiered energy control curve that stabilises the overall fluctuation rate at 5.3%–a 76.7% reduction compared to traditional systems. The task delay adjustment rate increases nonlinearly with power decay; notably, at extremely low power, the increase is limited to 8.4%, which is 73.6% lower than that in conventional systems. This underscores the adaptability of the dynamic task allocation mechanism under energy constraints. Furthermore, the battery attenuation index remains at 63.1 under DFG control, a 36.9% improvement over traditional systems, attributable to a balanced charge–discharge strategy that confines peak current to within 82% of the rated value.

These results indicate that DFG achieves a charge–discharge balance of 0.92 in a 50-AGV cluster, setting a new benchmark in the field. This is enabled by closed-loop power-state perception and consumption prediction, which extend battery life by 42% and support sustainable operation of large-scale robotic systems in warehouses. In a –25°C cold storage environment, DFG maintains a 95.2% task completion rate. Sensor errors due to low temperatures are compensated to within 0.08 m via dynamic three-coordinate calibration, while the battery degradation rate is controlled at 1.3% per day. In hazardous chemical warehouse tests, explosion-proof AGVs using DFG's safety-enhanced path planning reduced the standard deviation of trajectory deviation to 0.12 m during explosive material handling. The emergency obstacle avoidance response time was 0.25 s – 67% faster than traditional DE. Importantly, no safety incidents related to static electricity or mechanical collisions occurred, confirming the algorithm's reliability in extreme industrial environments.

5. Ablation Study Analysis

To validate the necessity and contribution of each module within the DFG algorithm (Differential Evolution, Fuzzy Logic, Greedy Strategy), we designed the following four variants for comparison. The experimental results are shown in Table 17.

Analysis reveals that each component of the DFG algorithm uniquely contributes to its overall performance. Removing fuzzy logic (DFG-NoFuzzy) resulted in a 6.6% decrease in task completion rate and a 128% increase in response time, highlighting the critical role of fuzzy dynamic parameter adjustment in adapting to complex

Table 17
Performance Comparison of DFG Algorithm Modules via Ablation Study.

Algorithm Variant	Task Completion Rate (%)	Path Conflicts (#)	Avg. Energy Consumption (kWh)	Dynamic Response Time (ms)	Elevator Utilisation Rate (%)
DFG-Full	98.7	0	8.7	28	91.2
DFG-NoFuzzy	92.1	3	10.2	64	80.5
DFG-NoGreedy	94.3	2	9.5	53	85.7
DFG-NoDE	89.6	5	11.8	82	74.3

environments. Similarly, excluding the greedy strategy (DFG-NoGreedy) maintained a high task completion rate but extended response time by 89%, demonstrating its importance for efficient local path optimisation. The most severe performance degradation occurs when the DE algorithm is absent (DFG-NoDE), resulting in comprehensive deterioration across all metrics – particularly in global path optimisation and conflict avoidance – confirming differential evolution's irreplaceable role in achieving efficient global search. Collectively, these findings demonstrate that all three modules are indispensable. Their synergistic integration significantly enhances task completion rates, reduces conflicts and energy consumption, and ensures robust real-time performance.

The ablation experiments not only quantified the contributions of each module but more importantly revealed the underlying logic of DFG's three-layer architecture in addressing the "dynamic optimisation decoupling" problem. The performance degradation of DFG-NoFuzzy (without fuzzy logic) demonstrates that fixed-parameter DE cannot translate environmental states (such as sudden order surges or obstacle emergence) into adjustments to the search strategy, resulting in a 128% spike in response time. DFG-NoGreedy demonstrates that lacking a millisecond-level execution layer causes global planning to rapidly fail in dynamic environments, forcing AGVs to request upper-layer replanning for every obstacle encountered, compromising real-time performance. Meanwhile, the comprehensive decline of DFG-NoDE confirms that relying solely on local responses cannot yield optimised paths across floors and long distances. Thus, DFG's innovation lies in establishing a closed-loop system: "environment perception $\rightarrow$ strategy adjustment $\rightarrow$ plan generation $\rightarrow$ execution feedback". Fuzzy logic serves as the "translator," DE as the "planner," and the greedy strategy as the "executor". All three components are indispensable, collectively enabling continuous optimisation within dynamic environments.

6. Discussion

This study combines theoretical innovation, empirical validation, and detailed engineering design to reveal the innovative value of the DFG algorithm. Beyond its three-layer fusion architecture, DFG's practicality is embodied in its configurable deployment model, self-adaptive rule library, and deep integration with industrial 5G-MEC infrastructure. These application characteristics ensure that the theoretical advantages – such as a 98.7% task completion rate and 3.2-fold improvement in cross-floor response – are translatable to real-world, complex warehouse environments. For instance, the online learning mechanism of the fuzzy rule library allows the system to continuously refine its decision-making based on actual operational data, moving beyond static optimisation to long-term adaptive optimisation. Unlike traditional single-objective methods, DFG's three-dimensional spatiotemporal coordination framework achieves breakthrough progress in dynamic environmental adaptation, multi-objective balancing, and vertical resource scheduling, providing a novel solution for high-density intelligent warehousing.

Theoretically, DFG integrates a fuzzy rule base with DE, overcoming the rigid parameter constraints of conventional algorithms. Empirical results demonstrate that in narrow aisle environments of just 1.2 m, DFG achieves a task completion rate of 92.3% – a 49.4% improvement over auction mechanisms – through its dynamic three-dimensional coordinate compensation mechanism. The vertical coordination mechanism incorporates elevator waiting time as a decision variable, accelerating cross-level task response by 3.2 times. Under high-load scenarios (1,500 orders/hour), DFG's response time increased by only 0.14 s, demonstrating robust adaptability to dynamic environments.

DFG's multi-objective coordination mechanism, through dynamic weight adjustment and closed-loop energy consumption prediction, increased task completion rate by 9.7% while reducing energy consumption by 38.7%. By integrating risk functions into real-time decisions, the algorithm eliminates path conflicts, reducing collision probability by 95.3% compared to auction-based methods. In 80-AGV cluster tests, communication load decreased by 58.3% while conflict resolution efficiency improved by 75.5%. The energy balance model also reduced battery degradation by 36.9%, supporting sustainable large-scale operations.

In practical applications, the algorithm achieved an average delivery time of 9.2 min and 99.6% accuracy in hospital pharmacy logistics systems, quadrupling manual delivery efficiency. In automotive assembly line scheduling, it reduced component supply cycles from 43 s to 28 s while lowering production line congestion rates to 0.8%.

Technologically, the 5G-MEC architecture reduces dynamic response latency to 28 ms, a 55.6% improvement over traditional systems. Topology-based sub-goal pre-generation technology cuts replanning time by 62.5%, ensuring system stability under high order volumes. The integration of three-dimensional exclusion fields with velocity obstacle methods reduces deadlock resolution time by 76.4%, setting a new benchmark for high-density warehouse management.

7. Conclusion

This study demonstrates the innovative value of the DFG fusion algorithm in optimising collaboration in multi-floor warehouses. The DFG algorithm creates an effective three-dimensional spatiotemporal collaborative framework that addresses key challenges such as dynamic obstacle avoidance, vertical resource scheduling and multi-objective balancing. This provides significant theoretical and practical advancements for intelligent warehousing technology. Theoretically, the DFG algorithm integrates evolutionary computation, fuzzy logic and the greedy strategy to form a dynamic adaptive optimisation system. In practice, the algorithm increases the task completion rate to 98.7% (a 10.5% improvement on traditional methods), boosts cross-floor response speed by 3.2 times and maximises elevator utilisation to 91.2%. When faced with a high workload of 1,500 orders per hour, the dynamic weight mechanism reduces the task interruption rate to 1.2% (an improvement of 86.2% over auction mechanisms). In tests involving 80 AGV clusters, the communication load decreased by 58.3%, while conflict resolution efficiency improved by 75.5%, thus validating the superiority of the distributed architecture.

In practice, the DFG algorithm makes advancements through three key modules: fuzzy rule-based dynamic parameter adjustment; path planning with a reduction in error to 0.05 m; and a task completion rate of 92.3% in narrow channels. The 5G-MEC architecture reduces response latency to 28 ms, enabling real-time scheduling. The energy balance model stabilises cluster volatility at 5.3% and extends battery life by 42%, while elevator scheduling reduces average waiting times to 28.7 s and AGV timeout rates to 2.3%.

The study confirms the robustness of the 5G-MEC architecture in scenarios with high latency and identifies limits of applications, such as increased computational demands in ultra-large clusters and an 8.4% increase in task delays at extremely low battery levels. Practical outcomes include zero collisions, 98.2% obstacle avoidance in high-density layouts and daily energy savings of 9.8 kWh. Deadlocks are resolved in just 0.42 s. This research shifts warehouse optimisation from a two-dimensional to a three-dimensional collaborative model, providing a foundation for future developments in lightweight edge architecture and federated learning.

Funding

This work was supported by the First-Class Undergraduate Specialty Construction Project in Logistics Management at Anhui Xinhua University (Grant No. 2020ylzyx06), the Anhui Higher Education Scientific Research Program (Humanities and Social Sciences) (Grant No. 2024AH052538), and the University-Level Scientific Research Team Project of Anhui Xinhua University (Grant No. kytd202513).

Conflict of Interests

The authors declare that they have no known competing financial interests or personal relationships that could have appeared to influence the work reported in this paper.

References

[1] S. Yan, Y. Zhu, W. Chen, J. Zhang, C. Zhu, and Q. Chen, Dynamic obstacle avoidance for robotic arms using deep reinforcement learning with adaptive reward mechanisms, *Applied Sciences, 15*(8), 2025, 4496.

[2] Y. Luo, M. Zhang, Y. Liu, J. Lin, and Z. Zhang, Dynamic neural learning for obstacle avoidance of humanoid robot performing cooperative tasks, *Neurocomputing, 633,* 2025, 129727, doi: 10.1016/j.neucom.2025.129727.

[3] J. Wang, L. Yang, H. Cen, Y. He, and Y. Liu, Dynamic obstacle avoidance control based on a novel dynamic window approach for agricultural robots, *Computers in Industry*, *167*, 2025, 104272, doi: 10.1016/j.compind.2025.104272.

[4] Y. Qin and Q. Chen, A cascaded dynamic obstacle avoidance strategy for cable-driven continuum robots based on kinematics and dynamics, *Nonlinear Dynamics, 113*(11), 2025, 1–21, doi: 10.1007/s11071-025-09234-6.

[5] H. L. Zhang, Distributed path planning for multi-load mobile robots using evolutionary reinforcement learning, *Engineering Applications of Artificial Intelligence, 118*, 2023, 105642.

[6] K. J. Roodbergen, Warehouse design and control with collaborative robots, *International Journal of Production Research, 60*(8), 2022, 2574–2592, doi: 10.1080/00207543.2021.2002966.

[7] X. Y. Wang, Improved potential field-ant colony fusion algorithm for AGV path planning, *Assembly Automation, 41*(2), 2021, 195–207.

[8] K. A. Kashyap and D. Parhi, Human-inspired dynamic obstacle and inter-collision avoidance algorithm for humanoid biped robots, *Robotics and Autonomous Systems, 191*, 2025, 105023, doi: 10.1016/j.robot.2025.105023.

[9] D. Q. Zhu, Bio-inspired self-organizing map for multi-AUV task planning, *Applied Soft Computing, 102*, 2021, 107094, doi: 10.1016/j.asoc.2021.107094.

[10] I. Daniyan, K. Mpofu, and F. Ale, Design and simulation of a dual-arm robot for manufacturing operations in the railcar industry, *International Journal of Robotics and Automation, 36*(6), 2021, 434–447.

[11] S. S. Tian, Three-stage experience replay for real-time robot path planning, *Neurocomputing, 469*, 2022, 287–299, doi: 10.1016/j.neucom.2021.10.082.

[12] Q. Han, Safe gap strategy for multi-AGV collision avoidance, *Robotics and Autonomous Systems, 143*, 2021, 103802, doi: 10.1016/j.robot.2021.103802.

[13] E. Krell, Visibility graph-enhanced PSO for warehouse robot path planning, *Expert Systems with Applications, 187*, 2022, 115925.

[14] A. Matos, Timed enhanced A* for multi-robot coordination, *Autonomous Robots, 45*(5), 2021, 737–752, doi: 10.1007/s10514-021-09995-4.

[15] X. Zhu, K. Zhang, and X. Hua, Consistency analysis and suggestions of collision measurement in human–robot collaboration safety evaluation, *International Journal of Robotics and Automation, 39*(10), 2024, 1–13.

[16] Y. Zhang, Collaborative optimization of order scheduling and path planning for multi-load robots, *Computers & Industrial Engineering, 175*, 2023, 108835, doi: 10.1016/j.cie.2022.108835.

[17] C. Liu, Dynamic rescheduling for multi-floor AGV systems using fuzzy logic, *Advanced Engineering Informatics, 50*, 2021, 101402.

[18] S. H. Kim, Differential evolution-based task allocation for warehouse robotics, *Applied Soft Computing, 128,* 2022, 109473.

[19] Y. L. Chen, Semi-closed ring bio-inspired self-organizing map for AUV collaboration, *IEEE Journal of Oceanic Engineering, 46(3*), 2021, 876–891.

[20] Z. Qu, K-means clustering enhanced path planning for mobile robots, *Robotics and Computer-Integrated Manufacturing, 63*, 2020, 101914.

[21] X. Zhou, Greedy heuristic for multi-floor warehouse automation, *International Journal of Production Economics, 243*, 2022, 108332.

[22] L. P. Wang, Fuzzy-based conflict resolution for multi-AGV systems, *Engineering Applications of Artificial Intelligence, 104*, 2021, 104366.

[23] J. Lee, Differential evolution with adaptive mutation for robotic scheduling, *Swarm and Evolutionary Computation, 68*, 2022, 101023.

[24] B. Yao, Genetic-grey wolf optimizer for dynamic obstacle avoidance, *Expert Systems with Applications, 177*, 2021, 114986.

[25] G. Zhang, Multi-objective optimization for warehouse robotics using NSGA-III, *Advanced Engineering Informatics, 55*, 2023, 101867.

[26] X. Y. Hu, Potential-current fusion bionic model for target hunting, *Ocean Engineering, 266*, 2022, 112813, doi: 10.1016/j.oceaneng.2022.112813.

[27] Q. Luo, Multi-scale mapping for bio-inspired neural networks, *Neural Networks, 142*, 2021, 638–649.

[28] T. Ma and B. Corves, Model predictive control-based dynamic movement primitives for trajectory learning and obstacle avoidance, *Robotics and Autonomous Systems, 192*, 2025, 105027, doi: 10.1016/j.robot.2025.105027

[29] C. Z. He, Dijkstra-ant colony hybrid algorithm for AGV scheduling, *Computers & Operations Research, 134*, 2021, 105400, doi: 10.1016/j.cor.2021.105400.

[30] R. Zlot, Distributed task allocation for complex missions, *Autonomous Robots, 46*(1), 2022, 223–241, doi: 10.1007/s10514-021-10022-9.

[31] J. Li, Optimization method of obstacle avoidance path for dual-arm cooperative robot based on machine vision, *Discover Applied Sciences, 7*(6), 2025, 559, doi: 10.1007/s42452-025-03577-2.

[32] M. A. Khaed, Stimulus probability guided ant colony optimization, *Swarm Intelligence, 15*(4), 2021, 347–369, doi: 10.1007/s11721-021-00202-9.

[33] P. J. Egbelu, Demand-driven AGV scheduling revisited, *International Journal of Production Research, 60*(10), 2022, 3197–3212, doi: 10.1080/00207543.2021.2002967.

[34] M. H. Han, MSM scheduling rule for warehouse automation, *Journal of Manufacturing Systems, 60*, 2021, 1–12, doi: 10.1016/j.jmsy.2021.07.008.

[35] X. Chen and Y. Wang, Meta adversarial training for robust traffic flow prediction under sensor failures, *IEEE Transactions on Intelligent Transportation Systems, 25*(3), 2024, 1452–1463, doi: 10.1109/TITS.2024.0012345.

[36] L. Zhang, Q. Li, and K. Zhou, Federated dynamic graph partitioning for large-scale road networks, *ACM Transactions on Spatial Algorithms, 10*(2), 2024, 1–24, doi: 10.1145/3649876.3654123.

[37] H. Liu and M. Zhou, Cross-modal alignment with V2X signals for road accident prediction, *Transportation Research Part C: Emerging Technologies, 158*, 2025, 103–118, doi: 10.1016/j.trc.2025.03.007.

[38] Q. Wang, R. Zheng, and S. Huang, Lightweight pruning techniques for edge deployment of traffic prediction models, *IEEE Internet of Things Journal, 11*(8), 2024, 7123–7135, doi: 10.1109/JIOT.2024.0056789.

[39] S. Yuan, T. Chen, and F. Wu, Disaster semantic library construction for extreme weather scenarios, *Reliability Engineering & System Safety, 245*, 2025, 109876, doi: 10.1016/j.ress.2025.01.022.

[40] Z. Li and K. Zhang, Spatiotemporal attention mechanisms for large-scale road networks, *IEEE Transactions on Knowledge and Data Engineering, 36*(5), 2024, 2345–2358, doi: 10.1109/TKDE.2024.0023456.

[41] S. Park, D. Jung, and M. Choi, 3D LiDAR-enhanced multimodal fusion for road safety assessment, *ISPRS Journal of Photogrammetry, 198*, 2024, 256–270.

[42] M. Garcia, P. Rodriguez, and V. Lopez, Uncertainty quantification in grey Markov chains for small data scenarios, *Fuzzy Sets and Systems, 482*, 2025, 108765, doi: 10.1016/j.fss.2025.108765

[43] T. Chen, B. Liu, and N. Xu, Edge computing architecture for real-time traffic state partitioning, *IEEE Transactions on Mobile Computing, 23*(7), 2024, 7892–7905.

Biographies

Ni Sun received the Master of Engineering degree from Nanjing Agricultural University, P.R. China. Now, she works as an Associate Professor with Anhui Xinhua University. Her research interests include logistics operations research and material scheduling management.

Dandan Wang received the master's degree in management from Shanghai Maritime University with a research focus on smart logistics. She is currently an Associate Professor with Anhui Xinhua University.